MAGNETIC FIELD DIFFUSION IN FAST DISCHARGING HOMOPOLAR MACHINES

M. D. Driga, E. B. Becker, R. D. Pillsbury,
W. F. Weldon, H. G. Rylander, and H. H. Woodson

Presented in the
Electric Machines and Electromechanics: An International Quarterly
October-December 1977

Publication No. PR-2
Center for Electromechanics
The University of Texas at Austin
Balcones Research Center
EME 1.100, Building 133
Austin, TX 78758-4497
(512)471-4496

MAGNETIC FIELD DIFFUSION IN FAST DISCHARGING HOMOPOLAR MACHINES

M. D. DRIGA, E. B. BECKER, R. D. PILLSBURY,* W. F. WELDON,
H. G. RYLANDER, and H. H. WOODSON

College of Engineering, The University of Texas at Austin

ABSTRACT

The unusually high mechanical and thermal stresses occuring in fast discharging homopolar machines require accurate prediction of high magnetic fields accompanying their operation. Linear methods and ideal configurations are no longer acceptable as simplifying assumptions in designing such devices used in controlled thermonuclear fusion experiments, laser applications, etc.

A finite element method - Galerkin technique is used for solution of Maxwell's equations for a moving medium. The transient skin effect in the system is described in terms of a magnetic vector potential and an electric scalar potential. Lagrange multipliers are used to impose the necessary constraint on the vector potential $\overline{A}$. The formulation for the steady-state magnetic fields in nonlinear media results as a particular case of the method.

This approach was used for predicting the parameters for the very fast discharging homopolar machine (FDX) designed by the Center for Electromechanics at The University of Texas at Austin. FDX is in an advanced state of fabrication.

INTRODUCTION

Fast discharging homopolar machines are an attractive solution for economically storing and transferring large amounts of energy. In some controlled thermonuclear experiments and laser applications they might represent the only feasible method.

The theory of fast discharging homopolar machines has been discussed in [1] and to a lesser degree in [2]. From the point of view of electromechanical energy conversion the ideal case of a piece of conductive material of unit volume, of density γ moving with velocity v in a magnetic field B is characterized by the discharge time

$$\tau_d = K_\tau \frac{\gamma v}{BJ} \qquad (1)$$

*Presently associated with Magnetic Corporation of America, Waltham, Mass.

Electric Machines and Electromechanics: An International Quarterly, 2:49-60, 1977

and the losses per unit volume

$$\lambda = K_\lambda \frac{\rho J}{Bv} \tag{2}$$

where ρ is the resistivity and (K_τ, K_λ) are constants. The reciprocal of the product

$$\tau_d \lambda \approx \frac{\rho\gamma}{B^2} \tag{3}$$

taken as a figure of merit for such a machine shows that a fast discharge with high efficiency is limited by the maximum attainable flux density and by the material which has the smallest $\rho\gamma$ product. Such a material - 7050 aluminum alloy - is used for the rotors of the FDX machine. Such an approach to the calculation of the fundamental parameters of a fast discharging homopolar machine, discharge time and efficiency, is elementary and incomplete. It does not take into account the topology of the machine (different parts of the rotor are in very different electromagnetic conditions and store different amounts of energy), or the compensation of armature reaction which affects the internal inductance and consequently the discharge time. The field diffusion into conductive parts of the machine can be taken into account considering the coefficients K_τ and K_λ as functions of discharge time which amounts to replacing simple relations (1), (2) with integral equations.

An equivalent circuit point of view is probably a more complete approach. A typical equivalent circuit for a fast discharge machine is shown in Fig. 1. The machine discharge is modelled by a complex R,L,C circuit in which $C_H = 4\pi^2 \frac{I}{\Phi^2}$ is the equivalent capacitance of the machine (I = moment of inertia, Φ = total flux linking the rotor) while the conductance GB parallel connected to C_H models the losses in bearings and windage. The FDX machine will be discharged initially in short circuit. The equivalent circuit valid for such a case is the same one but with the terminals X and y connected together.

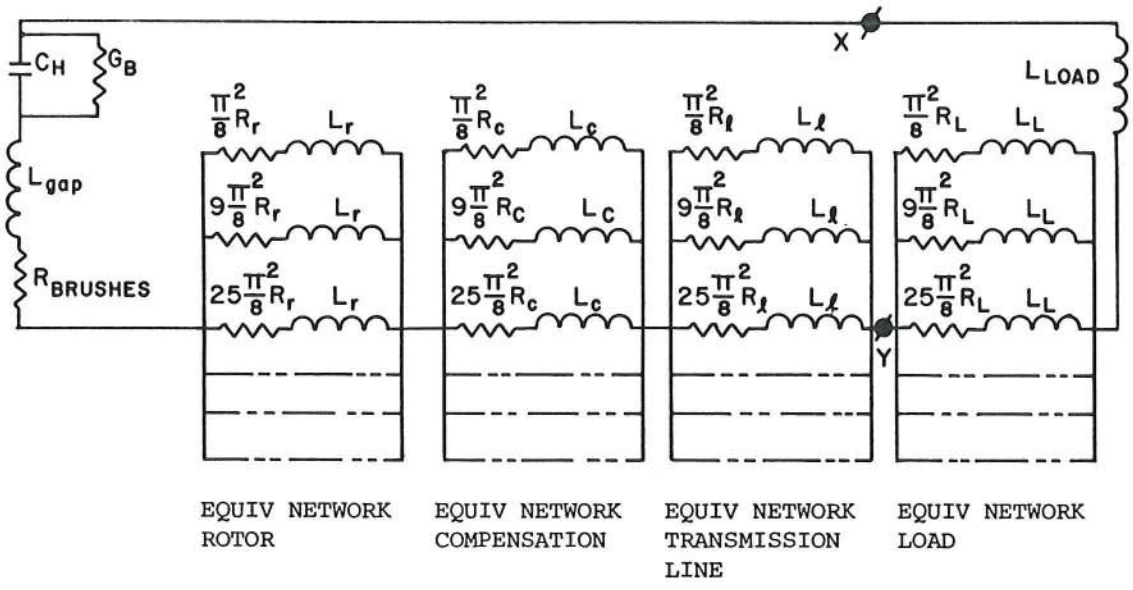

Figure 1: An Equivalent Circuit for a Fast Discharge Machine

The magnetic flux diffusion and current penetration are taken into account by introducing in the equivalent circuit a ladder network for each element of the machine, which, for achieving a minimum accuracy must contain a large number of elements characterizing a large number of "normal modes." Even then the results are not reliable for a good design because of the ideal shapes (i.e., infinite cylinders) and linearity of the differential equations implied by the network approach for transient skin effect. Due to the critical level of the mechanical and thermal stresses, brush current densities and interface speeds these simplifying assumptions are not appropriate; an exact numerical method is necessary.

Finite element methods have been widely used since 1970, in solving steady-state problems of magnetic fields, in complex, nonlinear systems [3,4,5]. In such situations the nonlinearity of the ferromagnetic materials is handled by linearizing the problem locally, solving the resulting linear equations and introducing the nonlinearity of the magnetization curve by an iterative correction to the linearized equations. Of course this assumes that the curve $B = f(H)$ is single-valued, neglecting hysteresis effects.

The solution of the diffusion of magnetic fields by a finite element method - Galerkin projective technique has been attempted in several papers [6,7]. Foggia et al. [6] assumed a steady-state harmonic regime and a prescribed sinusoidal traveling field impressed to the physical model. Miya [7] has a similar treatment prescribing the variation of plasma current in time. Actually it is not the solution for the forced response of the system but the solution for the "natural response" or rather the "complete response" that is required for pulsed power systems. The finite element method presented herein solves the transient diffusion problem in terms of a magnetic vector potential A through an intermediary electrokinetic scalar potential Ψ which transforms the forcing function concentrated in the generator into a distributed forcing function which acts locally in each point of the system: generator, transmission line, and load.

THE PHYSICAL PROBLEM

The physical problem treated herein is one of the several variants of the FDX experimental machine which is being built by the Center for Electromechanics at The University of Texas at Austin, in order to explore the fundamental limitations of fast dischargeing homopolar power supplies. A detailed account of the construction of the machine was presented in [2], and the experimental results will be the subject of a future paper. FDX is a fully compensated, pulsed field (4 Tesla in average) homopolar generator storing 0.36 MJ at 28,650 rpm in two counterrotating rotors. Figure 2 shows the machine configuration. Figure 3 gives the excitation flux lines in the rotor at the moment when the peak value of this flux is reached. The discharge current begins to flow initially in a very thin layer of the rotor and compensation plates, moments later penetrating into the interior of conductors.

The $J \times B_o$ forces stop the rotor, accelerate it in the opposite direction, stop it again until the stored energy is dissipated as joule and frictional losses (the machine is discharged in short circuit). Evaluation of the distribution in space and time of the transient electromagnetic fields and the accompanying stresses is the subject of this work.

THE MATHEMATICAL FORMULATION OF THE ELECTROMAGNETIC PROBLEM

For the time scale of the electromagnetic phenomena associated with the FDX the magneto-quasistatic approximation is used $\left(\underset{\sim}{J} >> \frac{\partial \underset{\sim}{D}}{\partial t}\right)$.

The energy stored at $t = 0$ in different parts of the system expressed through

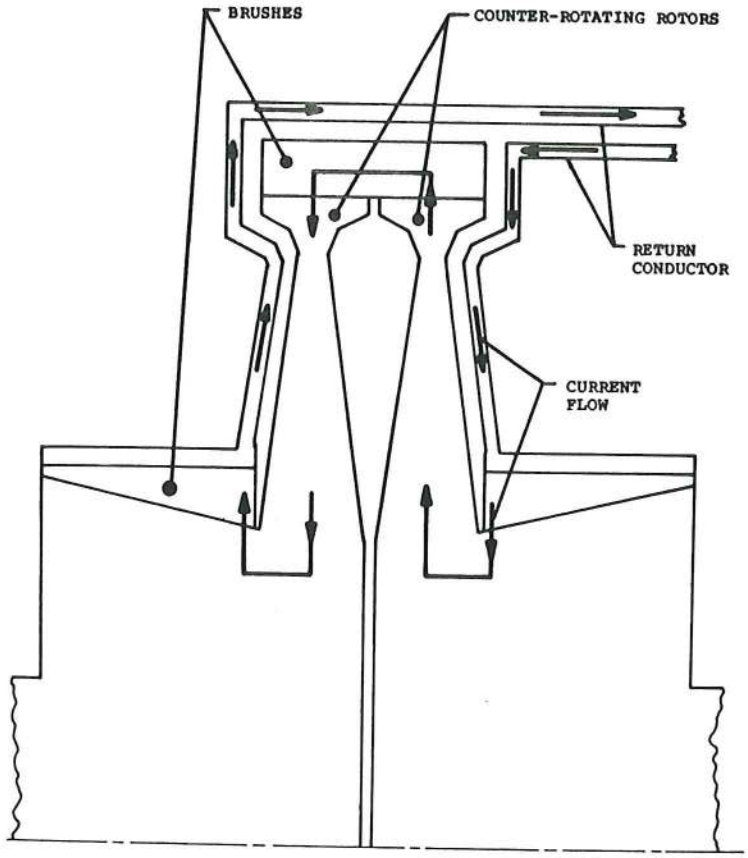

Figure 2. Machine Detail

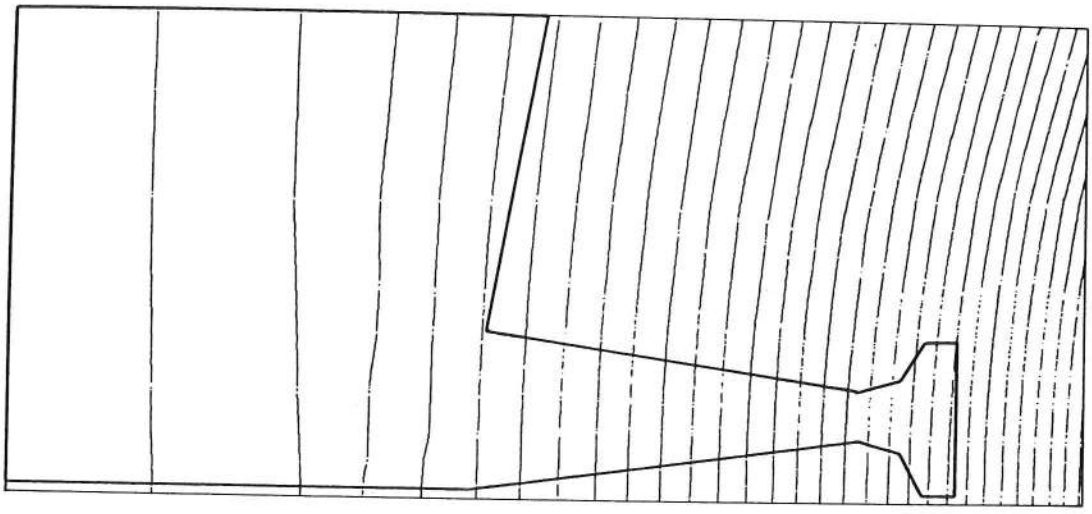

Figure 3: Magnetic Potential ($A_\theta r$) in Rotor

the electromagnetic state variable represents the input for Maxwell's equations. The "natural response" of this system is described by the solution sought through the finite element approach.

As mentioned before, previous treatments of the electromagnetic field diffusion [6,7] were seeking the "forced response" of the system. Boundary conditions were given at all times in such cases, and through them, for given material properties of the system - the electromagnetic field quantities were uniquely defined.

Maxwell's equations, for a magneto-quasistatic regime, can be written as

$$\begin{aligned} &(a) \quad \underset{\sim}{\nabla} \times \underset{\sim}{H} = \underset{\sim}{J} \\ &(b) \quad \underset{\sim}{\nabla} \times \underset{\sim}{E} = -\frac{\partial \underset{\sim}{B}}{\partial t} \\ &(c) \quad \underset{\sim\sim}{\nabla B} = 0 \end{aligned} \tag{4}$$

Ohm's law in moving media is given by

$$\underset{\sim}{J} = \sigma \left(\underset{\sim}{E} + \underset{\sim}{V} \times \underset{\sim}{B} \right) \tag{5}$$

and, in view of the assumption of homogenous, isotropic and hysteresis free materials

$$\underset{\sim}{B} = \mu \underset{\sim}{H} \tag{6}$$

In order to distribute the effects of the stored energy in the rotor characterized by the line integral of $\bar{V} \times \bar{B}$ as a variable of state, we introduce a scalar potential Ψ as an intermediate variable. At the moment of closing the switch, the electrokinetic state, characterized by Ψ is transmitted to each point of the closed electrical circuit.

This choice forces us to select as the primary independent variable the magnetic vector potential $\underset{\sim}{A}$, leading to

$$\underset{\sim}{E} = - \underset{\sim}{\nabla}\Psi - \frac{\partial \underset{\sim}{A}}{\partial t} \tag{7}$$

$$\underset{\sim}{B} = \underset{\sim}{\nabla} \times \underset{\sim}{A} \tag{8}$$

To these equations we adjoin the conditions that div $\underset{\sim}{J} = 0$, which expresses the conservation of charge condition and div $\underset{\sim}{A} = 0$. The last constraint is necessary ofr implementation of the magneto-quasistatic approximation and will be imposed through the use of Lagrange multipliers.

Substituting and combining the above equations yields the set

$$\begin{aligned} &\sigma \dot{\underset{\sim}{A}} + \underset{\sim}{\nabla} \times \frac{1}{\mu} \underset{\sim}{\nabla} \times \underset{\sim}{A} - \sigma(\underset{\sim}{V} \times \underset{\sim}{\nabla} \times \underset{\sim}{A} - \underset{\sim}{\nabla}\Psi) = \underset{\sim}{0} \\ &\underset{\sim}{\nabla} \cdot \sigma \underset{\sim}{\nabla}\Psi - \underset{\sim}{\nabla} \cdot \sigma(\underset{\sim}{V} \times \underset{\sim}{\nabla} \times \underset{\sim}{A} - \dot{\underset{\sim}{A}}) = 0 \end{aligned} \tag{9}$$

subject to

$$\underset{\sim}{\nabla} \cdot \underset{\sim}{A} = 0.$$

Because both the rotor motion $\underset{\sim}{V}$ and the potential of the applied magnetic field $\underset{\sim}{A}_o$ are axisymmetric and have only θ-components, the problem separates into two weakly coupled equations, (10) which governs the distribution of the steadily applied field and (9) which describes the transient skin effect

$$\underset{\sim}{\nabla} \times \frac{1}{\mu} \underset{\sim}{\nabla} \times \underset{\sim}{A}_o = \underset{\sim}{J}_o \tag{10}$$

The finite element solution of (10), although necessary to our problem, is a standard one [5] and need not be discussed further here.

In addition to the equations (9), we have as side conditions, the vanishing of the potentials at large distances from the conductors and the usual continuity or jump conditions on current and field. Because the current distributions do not extend to infinity:

$$A_r = A_z = \Psi = 0 \quad \text{as } r \to \infty \tag{11}$$

and

$$\underset{\sim}{n} \times \left[\!\!\left[\frac{1}{\mu}(\underset{\sim}{\nabla} \times \underset{\sim}{A}) \right]\!\!\right] = 0$$

$$\underset{\sim}{n} \cdot \left[\!\!\left[\sigma(\underset{\sim}{V} \times \underset{\sim}{\nabla} \times \underset{\sim}{A}_o - \underset{\sim}{\nabla}\Psi - \dot{\underset{\sim}{A}}) \right]\!\!\right] = 0 \tag{12}$$

In (12) the brackets denote the jump in the enclosed quantities across an interface between different materials or between moving and stationary materials. In the finite element model of the region shown in Figure 1, the symmetry about $r = 0$ and the antisymmetry about $z = 0$ give rise to the following additional boundary conditions

$$\begin{aligned} A_r &= 0 \qquad \text{on } r = 0 \\ A_r = \Psi &= 0 \qquad \text{on } z = 0 \end{aligned} \tag{13}$$

FINITE ELEMENT FORMULATION

We seek solutions to (9) and (12) subject to the conditions (11) and (13) in the weak or Galerkin sense. To this end we introduce [8] a Lagrange multiplier λ corresponding to the constraint (9c) and the test functions u, η, and τ corresponding to $\underset{\sim}{A}$, Ψ, and λ. The weak statement of the problem is

$$\Sigma_i \{ \iint_{\Omega_i} [\, \sigma \underset{\sim}{u} \cdot \dot{\underset{\sim}{A}} + \frac{1}{\mu} (\underset{\sim}{\nabla} \times \underset{\sim}{A}) \cdot (\underset{\sim}{\nabla} \times \underset{\sim}{u}) + \sigma \underset{\sim}{u} \cdot \underset{\sim}{\nabla}\Psi + \lambda \underset{\sim}{\nabla} \cdot \underset{\sim}{u} + \tau \underset{\sim}{\nabla} \cdot \underset{\sim}{A}$$

$$- \sigma \underset{\sim}{u} \cdot (\underset{\sim}{V} \times \underset{\sim}{\nabla} \times \underset{\sim}{A}_o) \,] \, da \} = 0 \tag{14}$$

and

$$\Sigma_i \{ \iint_{\Omega_i} [\, \sigma \underset{\sim}{\nabla}\eta \cdot \underset{\sim}{\nabla}\Psi + \sigma \dot{\underset{\sim}{A}} \cdot \underset{\sim}{\nabla}\eta - \sigma(\underset{\sim}{V} \times \underset{\sim}{\nabla} \times \underset{\sim}{A}_o) \cdot \underset{\sim}{\nabla}\eta \,] \, da \} = 0$$

for arbitrary $\underset{\sim}{u}$, η, and τ vanishing at ∞.

It is significant that the jump terms have equilibrated the boundary

integrals from the integration by parts, i.e. the jump conditions are natural conditions that follow from (14).

The discrete form of (14) is obtained by introducing the finite element approximation of the fields $\underset{\sim}{A}$, u, Ψ, η, λ and τ. The elements are quadrilaterals and the shape functions are quadratic for $\underset{\sim}{A}$, $\underset{\sim}{u}$, Ψ, and η and linear for λ and τ. Thus each corner node of the mesh has a total of four unknowns, i.e. A_r, A_z, Ψ and λ; while the midside nodes have only A_r, A_z, and Ψ. If the set of nodal point values is denoted $\underset{\sim}{q}$ then the discrete form of (14) can be written as

$$\underset{\approx}{C}\,\dot{\underset{\sim}{q}} + \underset{\approx}{K}\,\underset{\sim}{q} = \underset{\sim}{f} \tag{15}$$

In (15) C and K are, for an element, 28 x 28 matrices whose elements are the integrals of products of shape functions. It is apparent from (14) that neither C nor K is symmetric. The forcing function of f in (15) contains terms proportional to $\nabla \times \nu \times \underset{\sim}{A}_o$. The balance of energy is computed at each time step. By subtracting the volume integral of magnetic energy density ($B^2/2\mu$) and of specific ohmic loss (ρJ^2) from the kinetic energy initially stored in the rotor, a new speed V is obtained, a new forcing function is available for the next step. The value of the applied field $\underset{\sim}{A}_o$ is known from an initial finite element solution for the single component $A_{o\theta}$.

Although, in some designs, there is iron shielding around the field coil making the equations for $\underset{\sim}{A}_o$ nonlinear, the complete compensation of the machine as shown in Figure 1 confines the magnetic field governed by (15) to the region enclosed by the return conductor. There is no iron in the machine itself - the rotors being aluminum to reduce the discharge time of the machine - and so (15) is linear.

The initial value problem for $\underset{\sim}{q}$ is solved using a combination of algorithms. Using the approximation

$$\dot{\underset{\sim}{q}} = (\underset{\sim}{q}^{n+1} - \underset{\sim}{q}^{n})/\Delta t$$

leads either to

$$(\frac{2}{\Delta t}\,\underset{\approx}{C} + \underset{\approx}{K})\;\underset{\sim}{q}^{n+1/2} = \frac{2}{\Delta t}\,\underset{\approx}{C}\,\underset{\sim}{q}^{n} + \underset{\sim}{f}^{n+1/2} \tag{16}$$

or

$$(\frac{1}{\Delta t}\,\underset{\approx}{C} + \underset{\approx}{K})\;\underset{\sim}{q}^{n+1} = \frac{1}{\Delta t}\,\underset{\approx}{C}\,\underset{\sim}{q}^{n} + \underset{\sim}{f}^{n+1} \tag{17}$$

In (16) $\underset{\sim}{q}^{n+1/2} \equiv \frac{1}{2}\,(\underset{\sim}{q}^{n} + \underset{\sim}{q}^{n+1})$ is taken as the value at $(n + \frac{1}{2})\,\Delta t$. Both (16) and (17) are implicit and clearly each involves the same amount of computation. We find that, once started adequately, longer time steps can be used with (16) but that the use of (16) for the first few time steps leads to unacceptable noisy solutions. Since, with either scheme, a change in time step means reassembly and decomposition, there is no computational penalty paid in changing the scheme when the initial small time step is increased.

It is of great significance that, although neither C nor K is symmetric, $\beta C + K$ can be made symmetric simply by dividing the Ψ equations through by β. We have employed both symmetric band solvers and a frontal solver to reduce (16)

and (17).

A finite element program TEXMAP (Figure 4) solves the two weakly coupled problems mentioned above. The overlays EXTFLD and PENFLD solve the external magnetic field and the magnetic field penetration problems.

RESULTS

The first step in the analysis is to calculate the steady excitation field B_o in which the discharge takes place. The forcing function responsible for discharge (energy conversion and transfer), $[\underset{\sim}{V} \times \underset{\sim}{B}_o]$ has radial and axial components corresponding to the so-called "disk" and "drum" configurations of homopolar machines.

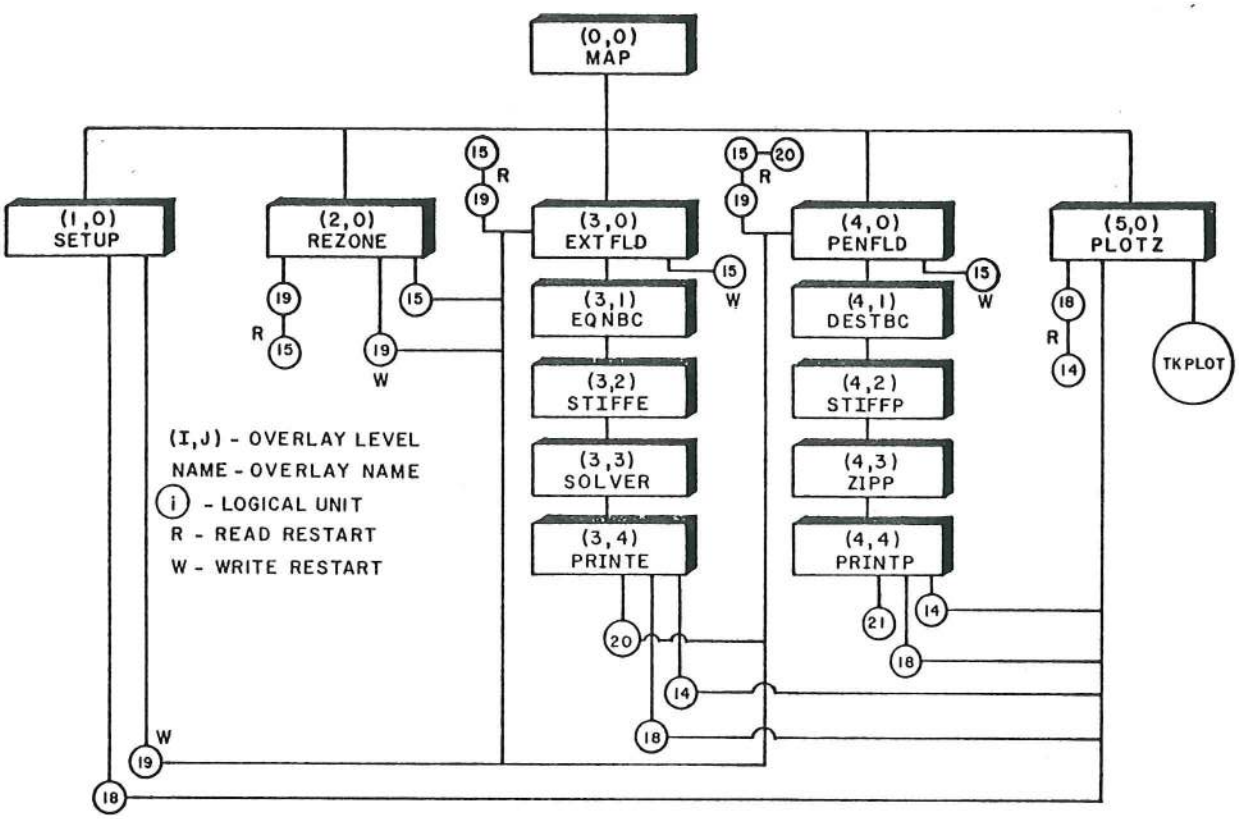

Figure 4: TEXMAP

The z component is very small when compared to the radial one but in the area covered by brushes it can cause important circulating currents along the rotor-brush interface (Figures 6-9).

Figures 6-9 show the contours of B_θ as time increases. (The current density of vector J with no component in the θ direction produces a flux density with only one component. J is tangent to the contours and its magnitude is inversely proportional to the distance between them.)

At 5 μsec all the current, hence all the field, is confined to the first

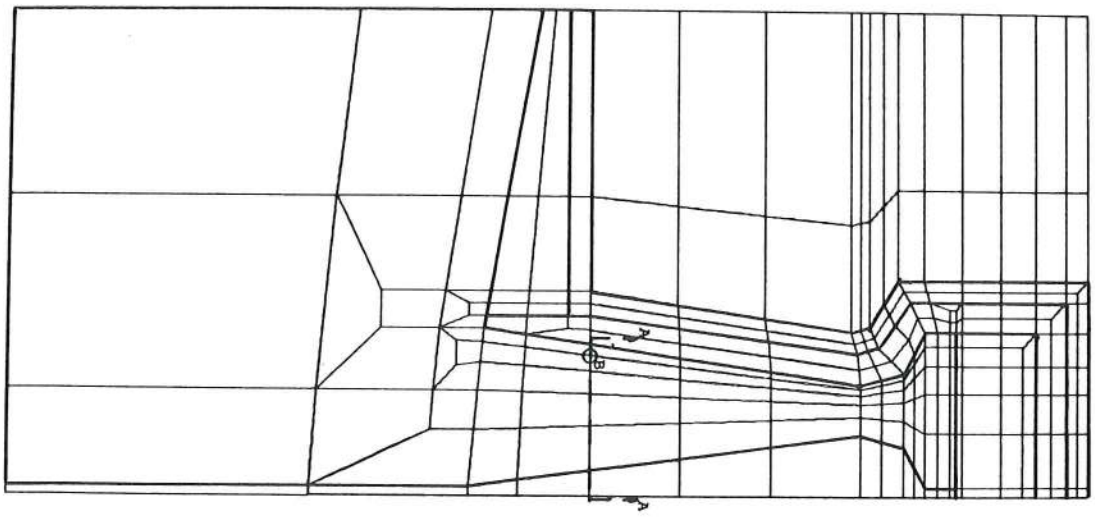

Figure 5: Finite Element Grid for the Machine

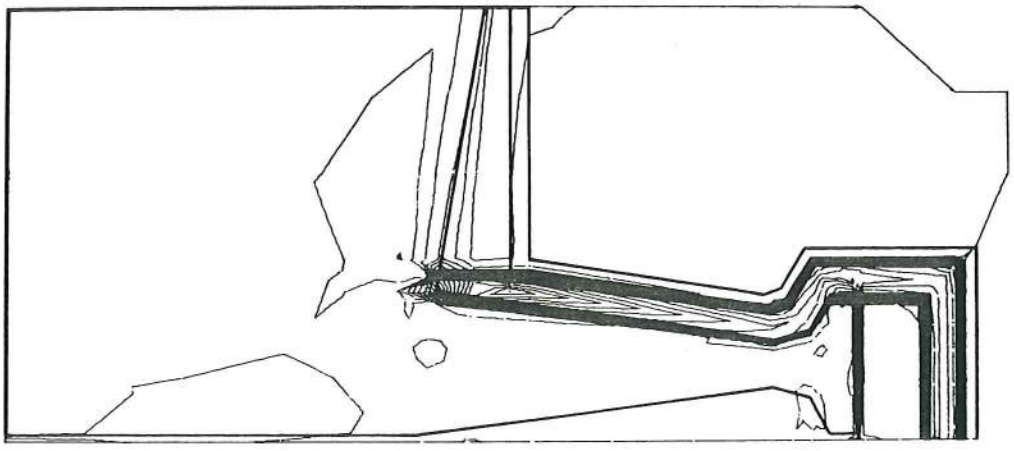

Figure 6: Magnetic Field B_θ t = 5 μsec

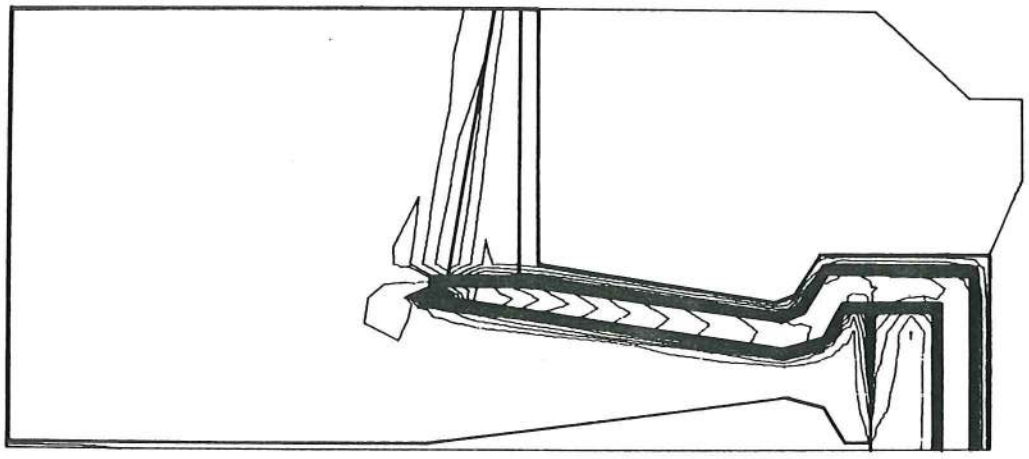

Figure 7: Magnetic Field B_θ t = 60 μsec

layer of elements adjacent to the airgap. Later (Figures 7-8) the current and field penetrate gradually - tending toward a uniform distribution. At the final time (Figure 9) the rotor has stopped and begins to reverse.

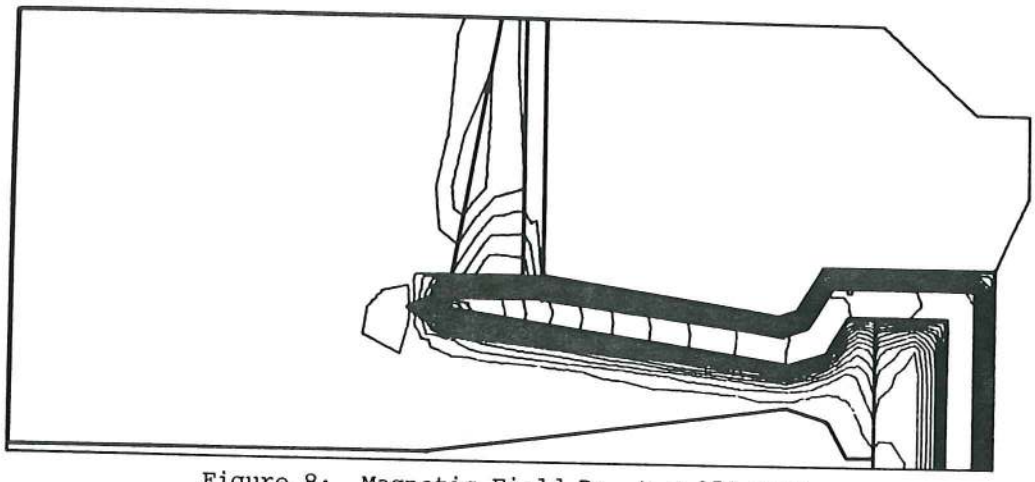

Figure 8: Magnetic Field B_θ t = 250 μsec

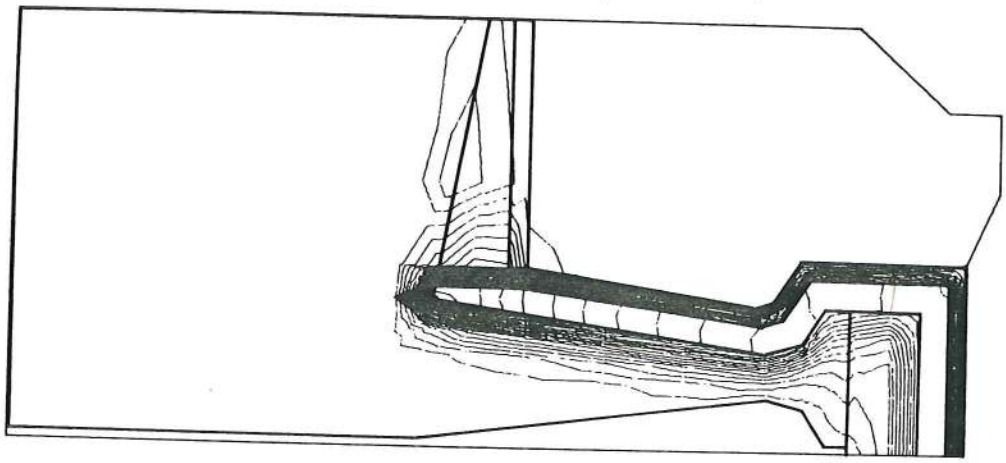

Figure 9: Magnetic Field B_θ t = 350 μsec

The J x B (N/m^3), electromagnetic force densities, are easily available from the field distributions. From them design parameters such as stresses as function of space and/or time (see Figure 10) can be calculated.

Design calculations for the FDX machine were based on the method outlined above. The FDX machine is in advanced state of fabrication (Figure 11) and final tests are expected to begin soon.

ACKNOWLEDGMENT

This work was supported by the Electric Power Research Institute (EPRI) and the Energy Research and Development Administration (ERDA).

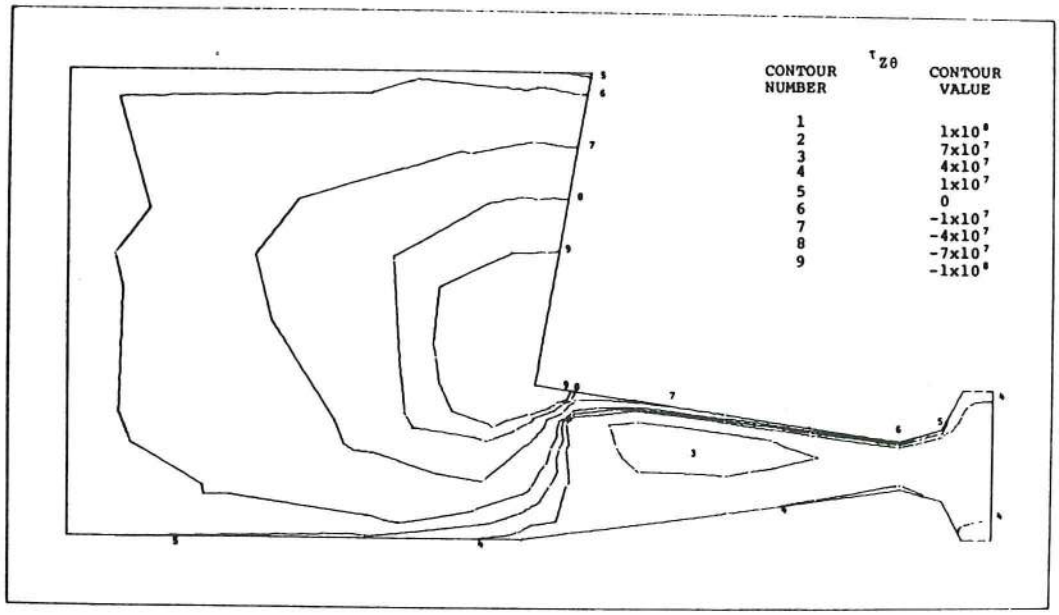

Figure 10: Contours of $\tau_{Z\theta}$ in the Rotor at Time t = 250 μsec

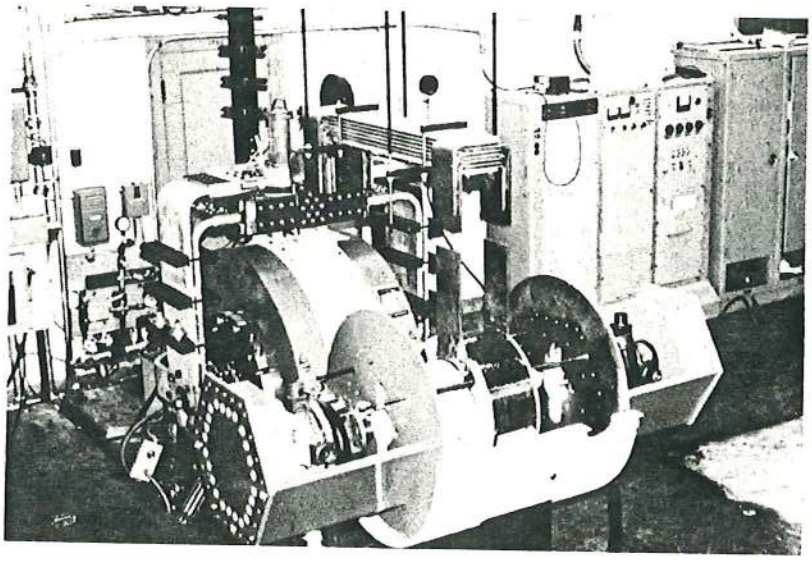

Figure 11: Photograph of FDX Machine

REFERENCES

1. M.D. Driga, S.A. Nasar, H.G. Rylander, W.F. Weldon and H.H. Woodson, "Fundamental limitations and topological considerations for fast discharge homopolar machines," IEEE Trans. on Plasma Science, vol. PS-3, No. 4, December 1975, pp. 209-215.

2. J.H. Gully, M.D. Driga, B. Grant, H.G. Rylander, K.M. Tolk, W.F. Weldon, H.H. Woodson, "One millisecond discharge time homopolar machine (FDX)," Proc. of IEEE International Conference on Pulsed Power Supplies, Lubbock, Texas, November 14-17, 1976

3. P. Silvester and M.V.K. Chari, "Finite-element solution of saturable magnetic field problems," IEEE Trans. on Power App. and Syst., vol. PAS 89, 1970, pp. 1642-1651.

4. M.V.K. Chari and P. Silvester, "Finite element analysis of magnetically saturated d.c. machines," IEEE Trans. on Power App. and Syst., vol PAS 90, 1971, pp. 2362-2372.

5. R. Glowinski and A. Marrocco, "Analyse numérique du champ magnetique d'un alternateur par éléments finis et sur-relaxation ponctuelle non linéaire," Computer Methods in Applied Mechanics and Engineering 3 (1974) pp. 55-85.

6. A. Foggia, J.C. Sabonnadiere and P. Silvester, "Finite element solution of saturated traveling magnetic field problems," IEEE Trans. on Power App. and Syst., vol. PAS-94, No. 3, 1975, pp. 866-870.

7. K. Miya, S. An, Y. Ando and Y. Suzuki, "Application of finite element method to electro-magneto-mechanical dynamics of superconducting magnetic coil and vacuum vessel," Proc. of the 6th Symposium on Engineering Problems of Fusion Research, San Diego, Cal., Nov. 1975.

8. R.H. Gallagher, "Finite element analysis fundamentals,"Prentice-Hall, Inc., Englewood Cliffs, New Jersey, 1975, pp. 196-199.

Manuscript received in final form, June 20, 1977